Article ID: 1003－6326(2003)01－0121－05

Electromagnetic separation of primary iron-rich phases from aluminum-silicon melt①

LI Tian-xiao(李天晓), XU Zhen-ming(许振明), SUN Bao-de(孙宝德),
SHU Da(疏 达), ZHOU Yao-he(周尧和)
(School of Materials Science and Engineering, Shanghai Jiaotong University, Shanghai 200030, China)

Abstract: The difference of conductivity between primary iron-rich phases and aluminum melt has been used to separate them by electromagnetic force (EMF) which is induced by imposing a direct electric current and a steady magnetic field in molten Al-Si alloy. Theoretical analysis and experiments on self-designed electromagnetic separation indicates that primary needle-like β phases are difficult to separate; while primary α iron-rich phases can be separated by electromagnetic separation. Primary iron-rich phases have been removed from the melt successfully when the molten metal flows horizontally through separation channel. The iron content is reduced from 1.13% to 0.41%.

Key words: aluminum-silicon melt; electromagnetic separation; primary iron-rich phase; removal efficiency
CLC number: TF 111.18; TF 114.12 **Document code:** A

1 INTRODUCTION

Iron is usually considered to be harmful impurity in aluminum. The needle-like or massive iron-silicon intermetallic compounds, are not only crack origins but also crack growth paths which dramatically influence the strength and elongation of aluminum alloy. These hard and brittle phases affect the surface property of material, too. Many researchers have suggested methods for reducing the detrimental effect of iron, such as gravity settlement[1], centrifugal method[2], addition of neutralization element[3-5], rapid solidification[6] and melt superheating[7,8]. Gravity settlement and centrifugal separation are difficult to apply to manufacturing systems because of low efficiency and non-continuous processing. Though neutralization element, rapid solidification and melt superheating can reduce the detrimental effect of iron-rich phases, these methods can not erase the deleterious effect completely.

Electromagnetic separation is a new method to remove primary iron-rich phases from aluminum melt with advantages of high efficiency, constant separation, causing no pollution on the melt which was studied scarcely. Park and Kim et al[9,10] studied electromagnetic separation of iron-rich phases from static aluminum melt. They got the result that the iron-rich phases can move to one side of separator. Continuous processing technique of this method and the influence of parameters and morphology of iron-rich phases on removal efficiency have not been reported[11].

In this research, removal efficiency of primary iron-rich phases and removal law have been studied. Primary phases formed by adding manganese have been removed by electromagnetic separation on a self-designed electromagnetic separation equipment continuously which provides a theoretical and technical basement for industrial application of this method.

2 THEORETICAL BACKGROUND

2.1 Forces exerted on iron-rich phases

The principle of electromagnetic separation is that EMF scarcely exerts on non-metallic phases due to different conductivity between aluminum melt and non-metallic phases, as a result, the non-metallic phases move in the direction opposite to that of EMF and are eliminated out of the melt. The net force exerted by the EMF field on a spherical particle can be expressed by Eqn. (1) according to Leenov and Kolin[9] in steady-state conditions and under the simplifying assumption that the fluid velocity is small:

$$\boldsymbol{F}_p = -\frac{3\sigma_f - \sigma_p}{2\sigma_f + \sigma_p}\frac{\pi d_p^3}{6}|\boldsymbol{J}\times\boldsymbol{B}| \quad (1)$$

where $\boldsymbol{F}_p$ is the net force exerted on the particle (electromagnetic repulsive force); σ_f, σ_p is electricity of aluminum melt and the particle; d_p is diameter of particle;

① **Foundation item:** Project(59871027) supported by the National Natural Science Foundation of China; project(G1999064900) supported by the National Key Fundamental Research and Development program of China
Received date: 2001－08－10; **Accepted date:** 2002－09－15
Correspondence: LI Tian-xiao, +86-21-62932030, txli@sjtu.edu.cn

$\boldsymbol{J}$ is the current density; and $\boldsymbol{B}$ is the magnetic flux density vector. Electricity of iron-rich phases can be considered to be zero relative to aluminum melt.

For long cylinder non-metallic particles, the force will depend on the orientation of the cylinder axis. Eqns. (2), (3) and (4) describe the electromagnetic repulsive force exerted on cylinder particles in three different cases: axis parallel to $\boldsymbol{B}$; parallel to $\boldsymbol{J}$; parallel to the force, hence perpendicular to $\boldsymbol{B}$ and $\boldsymbol{J}$.

$$\boldsymbol{F}_p = -\left(1-\frac{\sigma_p}{\sigma_f}\right) V|\boldsymbol{J}\times\boldsymbol{B}|$$

$$\boldsymbol{F}_p = -V|\boldsymbol{J}\times\boldsymbol{B}| \quad (2)$$

$$\boldsymbol{F}_p = \frac{2\sigma_p}{\sigma_f+\sigma_p} V|\boldsymbol{J}\times\boldsymbol{B}|$$

$$\boldsymbol{F}_p = 0 \quad (3)$$

$$\boldsymbol{F}_p = \frac{\sigma_f-\sigma_p}{\sigma_p+\sigma_f} V|\boldsymbol{J}\times\boldsymbol{B}|$$

$$\boldsymbol{F}_p = -V|\boldsymbol{J}\times\boldsymbol{B}| \quad (4)$$

where V is volume of the particle.

Except electromagnetic repulsive force, gravity, buoyance and drag resistance exert on iron-rich phases when the phases move in the melt in electromagnetic field. Drag resistance, R, can be calculated by

$$R = C_D \times A_p \times \frac{1}{2}\rho_f u_p^2 \quad (5)$$

where C_D is resistance coefficient, A_p is the area where drag resistance exerts on, u_p is velocity of iron-rich particle in the direction of electromagnetic repulsive force. ρ_f is the density of aluminum melt.

In order to separate primary iron-rich phases from aluminum melt, electromagnetic repulsive force and gravity should be in the same direction and perpendicular to the velocity of aluminum melt. When forces exerted on iron-rich particle reach balance, the velocity of iron-rich particle, u_p, reaches utmost velocity, u_∞, which is the terminal velocity.

$$C_D \times A_p \times \frac{1}{2}\rho_f u_\infty^2 = \left[\frac{3}{4}|\boldsymbol{J}\times\boldsymbol{B}| + (\rho_p-\rho_f)g\right] V \quad (6)$$

Therefore, the terminal velocity of particles can be calculated by Eqn. (7)[7]:

$$u_\infty = \frac{d_p^2}{24\mu}|\boldsymbol{J}\times\boldsymbol{B}| + \frac{gd_p^2}{18\mu}(\rho_p-\rho_f) \quad (7)$$

where μ is viscosity of the melt, ρ_p is the density of iron-rich phases.

2.2 Analysis of removal efficiency

The sketch of separator section is shown in Fig. 1. z-axis is in the flow direction of aluminum melt. If the flow of aluminum melt is even and constant, the velocity distribution of the melt can be expressed by

$$\frac{\partial^2 u}{\partial^2 x}+\frac{\partial^2 u}{\partial^2 y} = -\frac{g\lambda}{\nu} \quad (8)$$

Boundary conditions are

$$x = \pm b,\ u = 0,\ y = \pm h,\ u = 0 \quad (9)$$

where u is velocity of the melt, λ is head pressure loss of unit mass in unit flow path, ν is kinematic viscosity.

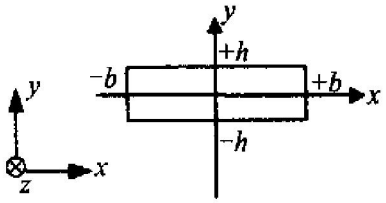

Fig. 1 Sketch of separator section

Hence the distribution of melt velocity is

$$u(x,y) = \frac{g\lambda}{2\nu}\left[(h^2-y^2)-\frac{32h^2}{\pi^3}\sum_{k=0}^{\infty}\left[\frac{(-1)^k}{(2k+1)^3}\frac{\mathrm{ch}\frac{(2k+1)\pi x}{2h}\cos\frac{(2k+1)\pi y}{2h}}{\mathrm{ch}\frac{(2k+1)\pi b}{2h}}\right]\right] \quad (10)$$

Value of z indicates the length of the separator EMF exerted on. Because diameter of iron-rich particles is small enough, velocity of particles in direction of z is equal to velocity of the melt, that is, $u_z = u(x,y) = \mathrm{d}z/\mathrm{d}t$, $u_y = u_\infty = \mathrm{d}y/\mathrm{d}t$, so that

$$\mathrm{d}z/\mathrm{d}y = u(x,y)/u_\infty \quad (11)$$

As one iron-rich particle gets to the edge of the separator ($y = -h$, $z = z$) which is considered to be captured and removed from the melt, its former position ($y = y$, $z = 0$) can be calculated by Eqn. (11). When this particle is captured, all iron-rich particles with the same diameter which are lower than this one at $z = 0$ are captured and removed from the melt. As a result, the removal efficiency can be expressed by the following equation:

$$\eta = \int_{-h}^{h}\int_{-b}^{b} u(x,y)\,\mathrm{d}x\,\mathrm{d}y \Big/ \int_{-h}^{h}\int_{-b}^{b} u(x,y)\,\mathrm{d}x\,\mathrm{d}y \quad (12)$$

According to Eqn. (11) and Eqn. (12), one value of z can get one y and one y can get one η so that different lengths of the separator EMF exerted on result in different removal efficiencies.

Numerical integration of Eqn. (11) and Eqn. (12) is difficult and can not get clear relationship between the parameters and removal efficiency. For rectangle of large ratio of width to height, the velocity distribution of the melt can be simplified to be

$$u_z = u_M\left[1-\left(\frac{y}{h}\right)^2\right] \quad (13)$$

where u_M is the maximum velocity of the melt. Therefore, numerical integration of Eqn. (12) is

$$\eta = \int_{-h}^{h} u_M\frac{h^2-y^2}{h^2}\mathrm{d}y \Big/ \int_{-h}^{h} u_M\frac{h^2-y^2}{h^2}\mathrm{d}y$$

$$\eta = \frac{3h^2y - y^3 + 2h^3}{4h^3} \quad (14)$$

Numerical integration of Eqn. (11) is:

$$\int_0^z dz = \int_h^h u_M \frac{h^2 - y^2}{h^2} dy$$

$$z = -\frac{3h^2y - y^3 + 2h^3}{3h^2} \cdot \frac{u_M}{u_\infty} \quad (15)$$

The density of iron-rich phases is (3.35 ~ 3.45) × 10^3 kg/m^3 and the density of the melt is 2.4 × 10^3 kg/m^3. In most electromagnetic separation, EMF is larger than 1 × 10^5 N/m^3. Therefore, the influence of gravity on the velocity of iron-rich particles can be neglected so that η can be calculated by

$$\eta = \frac{3zBI}{8hu_f} \cdot \frac{d_p^2}{24\mu} \quad (16)$$

where $u_f = 0.5\ u_M$ is average velocity of the melt. It is seen that removal efficiency increases with the increase of EMF and diameter of iron-rich particles and decreases with the increase of velocity of the melt and height of separator.

3 EXPERIMENTAL

Al-12% Si-1% Fe-0.6% Mn and Al-12% Si-1.1% Fe-1.2% Mn were chosen. The removal efficiency is examined by observing metallographs of the metal before and after electromagnetic separation and by the LECO image analysis system equipped with an optical scope. The removal procedure of iron-rich phases was illustrated in Fig. 2. The whole separator was made of fire-resistant material. The section of the separator in the range of electromagnetic field was rectangle. An electromagnet was used to generate the desired normal magnetic field. The magnetic flux density was measured by a Gauss meter to be 0.94 T. A DC generator was used to support DC current for the melt. The electric current density was adjusted by changing the current and the section of the separator. The velocity of the melt was measured by quantifying the melt flown out of the separator within a certain interval.

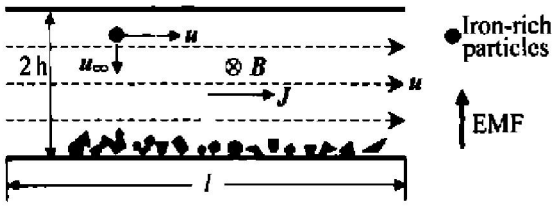

Fig. 2 Sketch of movement and enrichment of iron-rich phases in separator

The experiment mainly involved melting and electromagnetic separating on self-designed equipment. The experimental alloy was melted and kept at 640 ℃ for 30 min to form primary iron-rich phases. The melt was stirred to make iron-rich phases uniform before electromagnetic separation. After the experiment, the solidified metal before being processed, in the separator and after being processed was examined metallographically and by image analysis to determine content of primary iron-rich particles in the metal and the particle distribution on the across section of the separator. Iron content of the alloy before and after electromagnetic separation was measured by chemical analysis.

4 RESULTS AND DISCUSSION

Fig. 3 shows the microstructures of Al-12% Si-1% Fe-0.6% Mn before and after electromagnetic separation. Experimental parameters were: EMF 1.73 × 10^5 N/m^3, velocity of the melt 16.4 mm/s, section gauge of the separator 11 mm × 16 mm. It can be seen that there were many α (massive iron-rich particles) and β (needle-like) iron-rich phases in the alloy before electromagnetic separation and there were many β iron-rich phases but no massive primary α iron-rich phases in the melt after separation. It indicated that electromagnetic separation can not remove iron-rich phases efficiently because of β iron-rich phases was not large enough when ratio of Mn to Fe keeps content (Mn/Fe). When axis of needle-like iron-rich

Fig. 3 Microstructures of Al-Si alloy before and after electromagnetic separation
(a) —Before electromagnetic separation;
(b) —After electromagnetic separation
(Corroded in 20% H_2SO_4 at 70 ℃, iron-rich phases are black)

phases is parallel to $\boldsymbol{B}$, to $\boldsymbol{J}$ and to EMF, electromagnetic repulsive force exerted on the phases is different according to Eqns. (2), (3) and (4). Because orientation of needle-like phases in the melt is random, the repulsive force is not uniform, so only some needle-like phases whose orientation is suitable to electromagnetic separation can be removed from the melt. In addition, formation of needle-like phases is in the end of solidification and viscosity of the melt during this period is large so β iron-rich phases are difficult to be removed.

Fig. 4 shows the microstructures of Al-12% Si-1.1% Fe-1.2% Mn before and after electromagnetic separation. Experimental parameters were: EMF

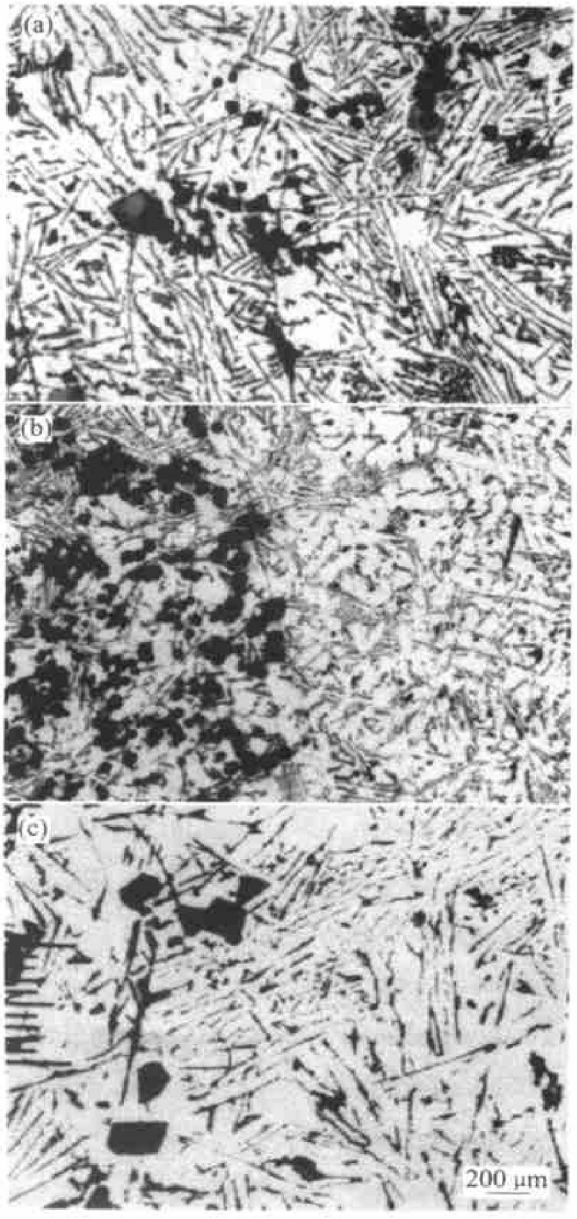

Fig. 4 Microstructures of Al-Si alloy before and after electromagnetic separation
(a) —Before electromagnetic separation;
(b) —Distribution of iron-rich phases in separator;
(c) —After electromagnetic separation
(Corroded in 20% H_2SO_4 at 70 ℃, iron-rich phases are black)

2.12×10^5 N/m^3, velocity of the melt 41.6 mm/s, section gauge of the separator 8 mm × 18 mm. It can be found in Fig. 4(a) that there are more primary α iron-rich phases than that in Fig. 3(a) but no β iron-rich phases exist when Mn/Fe is larger than 1. There were no primary iron-rich phases in the alloy after electromagnetic separation (α and β) indicated by Fig. 4(c). Fig. 4(b) is the distribution of primary iron-rich phases in the separator. Fig. 4 shows that primary iron-rich phases moved to one side of the separator and were captured, so the melt flew out of the separator was free of primary iron-rich phases.

Two separating experiments have been done to check the effectiveness of electromagnetic separation of primary iron-rich phases. The alloy is chosen to be Al-12.23% Si-1.13% Fe-1.22% Mn. Experimental parameters in the two experiments were: EMF 1.4×10^5 N/m^3, velocity of the melt 51.7 mm/s, section gauge of the separator 9 mm × 16 mm and EMF 8.7×10^5 N/m^3, velocity of the melt 121.3 mm/s, section gauge of the separator 5 mm × 19 mm, respectively. Chemical analysis indicated that content of Mn and Fe are 0.69% and 0.77%, respectively, in the alloy processed by the first mentioned experiment; while they are 0.26% and 0.41% processed by the second experiment. The size and content of primary α iron-rich phases in the alloy before and after electromagnetic separation analyzed by LECO Image Analyzer showed that there are many primary iron-rich phases in the alloy processed by the first experiment; while there are no primary iron-rich phases larger than 20 μm in the alloy processed by the second experiment. Removal efficiency of 30 μm iron-rich phases was calculated to be 40.6% by Eqn. (16) according to the parameters in the first experiment; while removal efficiency of 20 μm iron-rich phases was 100% according to the parameters in the second experiment. It indicated that theoretical analysis of removal efficiency is almost the same as experimental measurement. The experiments and theoretical analysis showed that large EMF and small height of the separator are advantageous to the remove of primary iron-rich phases.

5 CONCLUSIONS

1) Needle-like β iron-rich phases are difficult to be removed from the melt by electromagnetic separation; while primary α iron-rich phases can be removed by this method.

2) The iron content of Al-Si alloy can be reduced from 1.13% to 0.41% by electromagnetic separation.

3) The experimental result is the same as theoretical analysis.

REFERENCES

[1] Shabestari S G, Grzleski J E. Gravity segregation of complex intermetallic compounds in liquid aluminum-silicon alloys[J]. Mater Trans A, 1995, 26A(4): 999-1006.

[2] Hiromi Matsubara, Norihisa Izawa. Macroscopic segregation in Al-11% Si alloy containing 2% Fe(mass fraction) solidified under centrifugal force[J]. Journal of Japan Institute of Light Metals, 1998, 48(2): 93-97.

[3] Murali S, Raman K S, Murthy K S S. Morphological studies on β-$FeSiAl_5$ phase in Al-7Si-0.3Mg alloy with trace additions of Be, Mn, Cr, and Co[J]. Materials Characterization, 1994(33): 99-112.

[4] Couture A. Iron in aluminum casting alloys—a literature survey[J]. AFS Transactions, 1981(11): 9-17.

[5] HUANG Shang-yu, CHANG Zhi-hua, WANG Zhong-ren, et al. A finite-element analysis of electromagnetic sheet metal-expansion process[J]. Trans Nonferrous Met Soc China, 1998, 8(3): 490-495.

[6] Avano Y, Shimizu Y. Non-equilibrium crystallization of AlFeSi compound in melt-superheated Al-Si alloy castings [J]. AFS Transactions, 1990(98): 889-895.

[7] Narayanan L A, Samuel F H, Gruzleski J E. Crystallization behavior of iron-containing intermetallic compounds in 319 aluminum alloys[J]. Mater Trans A, 1992, 25A(8): 1761-1773.

[8] CAO Zhi-qiang, ZHANG Xing-guo, JIN Jun-ze. Measurement and analysis of magnetic fields of electromagnetic casting alloy[J]. Trans Nonferrous Met Soc China, 1996, 6(1): 100-105.

[9] Park Joon-Pyou, Sassa K, Asai A. Elimination of iron in molten Al-Si alloys by electromagnetic force[J]. Journal of Institute of Metals, 1995, 59(3): 312-318.

[10] Kim Jeong-Ho, Yoon Eui-Pak. Elimination of Fe element in A380 aluminum alloy scrap by electromagnetic force[J]. Journal of Materials Science Letters, 2000(19): 253-255.

[11] MAO Da-heng, XIAO Li-long. Effects of electromagnetic field on casting-rolling strips breakdowns[J]. Trans Nonferrous Met Soc China, 1997, 7(4): 5-11.

[12] Daniel Leenov, Alexander Kolin. Theory of electromagnetophoresis (Ⅰ)—magnetohydrodynamic forces experienced by spherical and symmetrically oriented cylindrical particles [J]. The Journal of Chemical Physics, 1954, 22(4): 683-688.

(Edited by HUANG Jin-song)